

Supplementary Information

Sterically Congested Pyrrole-Fused Tetrathiafulvalene Decamers as Highly Conductive Amorphous Molecular Materials

Masayoshi Takase,* Naofumi Yoshida, Tomoyuki Narita, Takashi Fujio, Tohru Nishinaga, and
Masahiko Iyoda*

Department of Chemistry, Graduate School of Science and Engineering, Tokyo Metropolitan University, Hachioji, Tokyo 192-0397, Japan,
E-mail: mtakase@tmu.ac.jp, iyoda@tmu.ac.jp

Contents

S1. Material and methods	... p.S2
S2. ^1H and ^{13}C NMR spectra	... p.S4
S3. Chemical oxidations of 4b	... p.S6
S4. XRD patterns and SEM images of self-assembled 4b and their conductivities	... p.S7
S5. Single crystal structure of 5	... p.S8
S6. DFT calculations of decafluorobiphenyl and 4b	... p.S10
S9. References	... p.S14

S1. Material and methods

¹H and ¹³C NMR spectra were recorded on Bruker 500 spectrometer with use of tetramethylsilane proton or carbon signal as an internal standard. Electron impact (EI) mass spectra and laser desorption ionization time-of-flight (LDI-TOF) mass spectra were obtained on SHIMADZU GC-MS QP2020 and AXIMA-CFR, respectively. Melting points were determined with Yanako MP-500D and not corrected. Elemental analyses were performed with Exeter Analytical, Inc. CE-440F. Column chromatography was carried out using Merck silica gel 60, Daiso silica gel 1001W, or neutral alumina activity II-III, 70-230 mesh ASTM. Gel permeation chromatography (GPC) was performed using a JAI model LC-908 recycling preparative HPLC equipped with JAIGEL-1H-40 and -2H-40 columns (40 x 600 mm) with toluene as eluent. Differential scanning calorimetry (DSC) and thermogravimetric analysis (TGA) was carried out with Rigaku DSC8230L under nitrogen atmosphere. Absorption spectra were recorded on SHIMADZU UV-Vis-NIR scanning spectrophotometer (Model UV-3101-PC). Cyclic voltammetry (CV) and differential pulse voltammetry (DPV) measurements were performed on BAS-ALS620B electrochemical analyzer using a standard three-electrode cell consisting of Pt working electrodes, a Pt wire counter electrode, and a Ag/AgNO₃ reference electrode under nitrogen atmosphere. The potentials were calibrated with ferrocene as an external standard. Atomic force field microscopy (AFM) and scanning electronic microscopy (SEM) measurements were carried out with KEYENCE, Nanoscale Hybrid Microscope VN-8000 (tapping mode) and KEYENCE VE-9800, respectively. Electric conductivity measurements were performed with Advantest R6551 Digital Multimeter. All reactions were carried out under nitrogen atmosphere. THF was freshly distilled from sodium benzophenone ketyl before use, and other solvents were purified with standard methods.

Synthetic Methods

Decakis[2-(4,5-bis(butylthio)-1,3-dithiol-2-ylidene)-(1,3)-dithiolo[4,5-*c*]-N-pyrrolyl]biphenyl (**4b**)

To a DMF-THF (5 + 5 mL) solution of **6** (303 mg 0.72 mmol) was added NaH (60% oil dispersion, 33 mg, 0.83 mmol) at 0 °C. After stirring for 30 min at the same temperature, decafluorobiphenyl (12 mg, 0.36 mmol) was added. The reaction mixture was allowed to warm to room temperature over 9 hours, and then it was heated up to 70 °C and stirred for 3 hours. After addition of H₂O, the aqueous phase was extracted by THF, and then combined organic phase was washed with brine, and dried over MgSO₄. Concentration in vacuo gave a dark oil, which was subjected to column chromatography (Al₂O₃; eluent, CH₂Cl₂) and GPC (eluent, toluene), and re-crystallized from CH₂Cl₂ and hexane to give **4b** as a dark-yellow solid in 44% yield (67 mg, 0.016 mmol). dec. > 226 °C; ¹H NMR (500 MHz,

CDCl_3) δ 5.98 (s, 4H), 5.86 (s, 8H), 5.65 (s, 8H), 2.84-2.79 (t, J = 7.3 Hz, 40H), 1.68-1.58 (m, 40H), 1.44-1.39 (m, 40H), 0.97-0.89 (m, 60H); ^{13}C NMR (125 MHz, CDCl_3) δ 132.35, 127.64, 127.52, 126.56, 125.17, 124.96, 124.42, 117.70, 117.46, 115.18, 114.86, 112.27, 112.15, 111.99, 111.72, 111.66, 36.04, 35.99, 31.76, 21.73, 21.70, 21.67, 13.68, 13.64; UV-vis ($\text{CH}_2\text{Cl}_2/\text{CH}_3\text{CN}$ 2:1) λ_{\max} nm (log ϵ) 298 (4.65), 322 (4.59), 370 (4.21); LDI-TOF-MS: calcd for MH^+ , $\text{C}_{172}\text{H}_{200}\text{N}_{10}\text{S}_{60}$: 4329.9; found 4331.5. Anal. Calcd for $\text{C}_{172}\text{H}_{200}\text{N}_{10}\text{S}_{60}$: C, 47.69; H, 4.65; N, 3.23. Found: C, 47.98; H, 4.72; N, 3.20.

Decakis(*N*-pyrrolyl)biphenyl (**5**)

To a DMF (20 mL) solution of pyrrole (679 mg 10.0 mmol) was added NaH (60% oil dispersion, 420 mg, 10.5 mmol) at 0 °C. After stirring for 30 min at the same temperature, decafluorobiphenyl (167 mg, 0.50 mmol) was added. The reaction mixture was heated up to 80 °C and stirred for overnight. After addition of H_2O , the aqueous phase was extracted by ether, and then combined organic phase was washed with brine, and dried over MgSO_4 . Concentration in vacuo gave a pale-yellow solid, which was subjected to column chromatography (SiO_2 ; eluent, Hexane: CH_2Cl_2 = 2: 3) and crystallized from CH_2Cl_2 and hexane to give **5** as colorless prisms in 96% yield (378 mg, 0.47 mmol). dec. > 311 °C; ^1H NMR (500 MHz, CDCl_3) δ 6.08 (dd, J = 2.1, 2.1 Hz, 4H), 6.03-5.98 (m, 28H), 5.96 (dd, J = 2.2, 2.2 Hz, 8H); ^{13}C NMR (125 MHz, CDCl_3) δ 136.89, 136.46, 133.53, 127.57, 121.46, 120.87(2C), 110.55, 110.40, 109.86; EI-MS: calcd for M^+ , $\text{C}_{52}\text{H}_{40}\text{N}_{10}$: 804.3; found 804.; Anal. Calcd for $\text{C}_{52}\text{H}_{40}\text{N}_{10}$: C, 77.59; H, 5.01; N, 17.40. Found: C, 77.20; H, 4.74; N, 17.22.

S2. ^1H and ^{13}C NMR spectra

Figure S2-1. ^1H NMR of **4b** (CDCl_3 , 500 MHz)

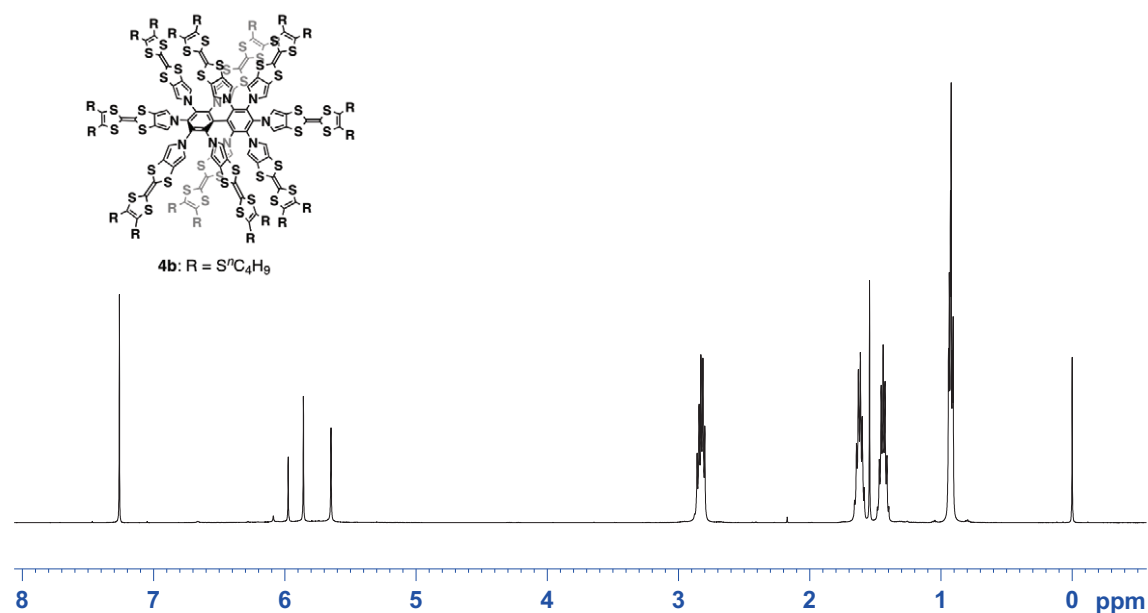


Figure S2-2. ^{13}C NMR of **4b** (CDCl_3 , 125 MHz)

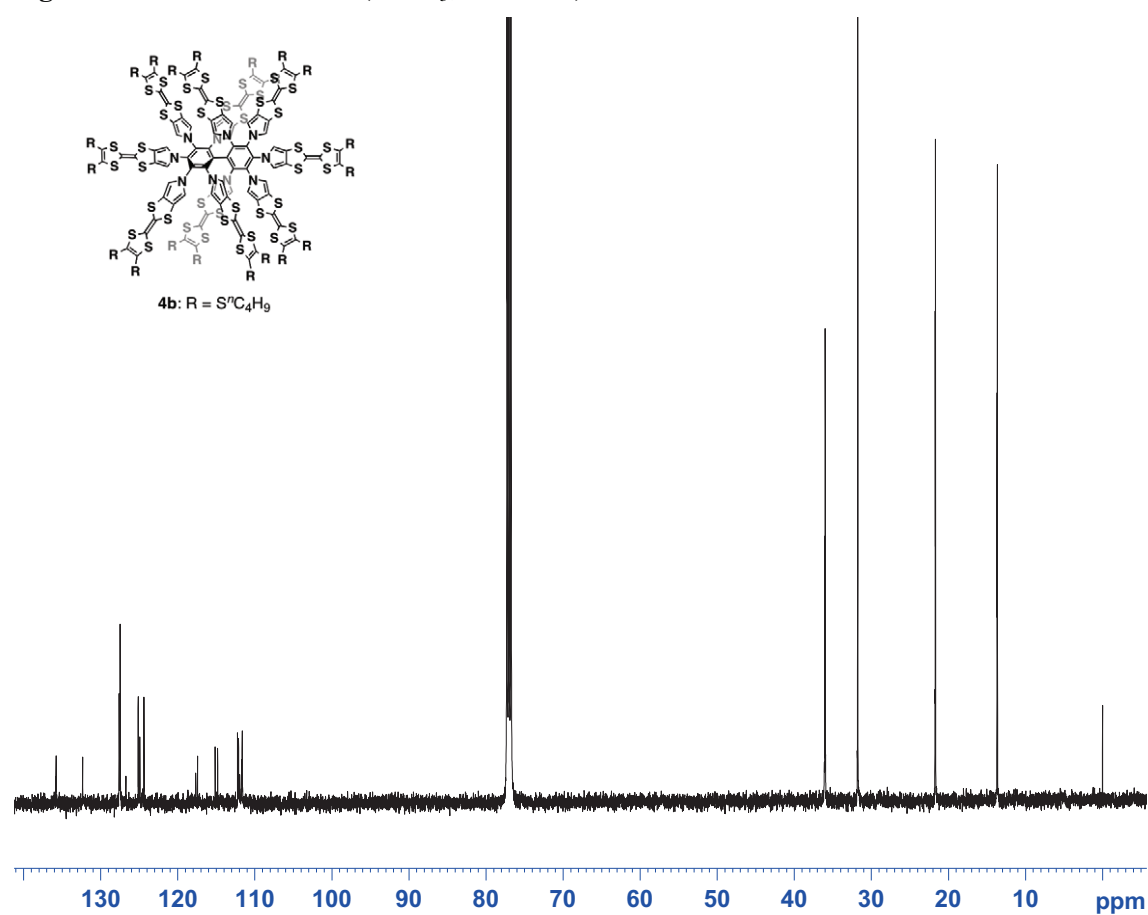


Figure S2-3. ^1H NMR of **5** (CDCl_3 , 500 MHz)

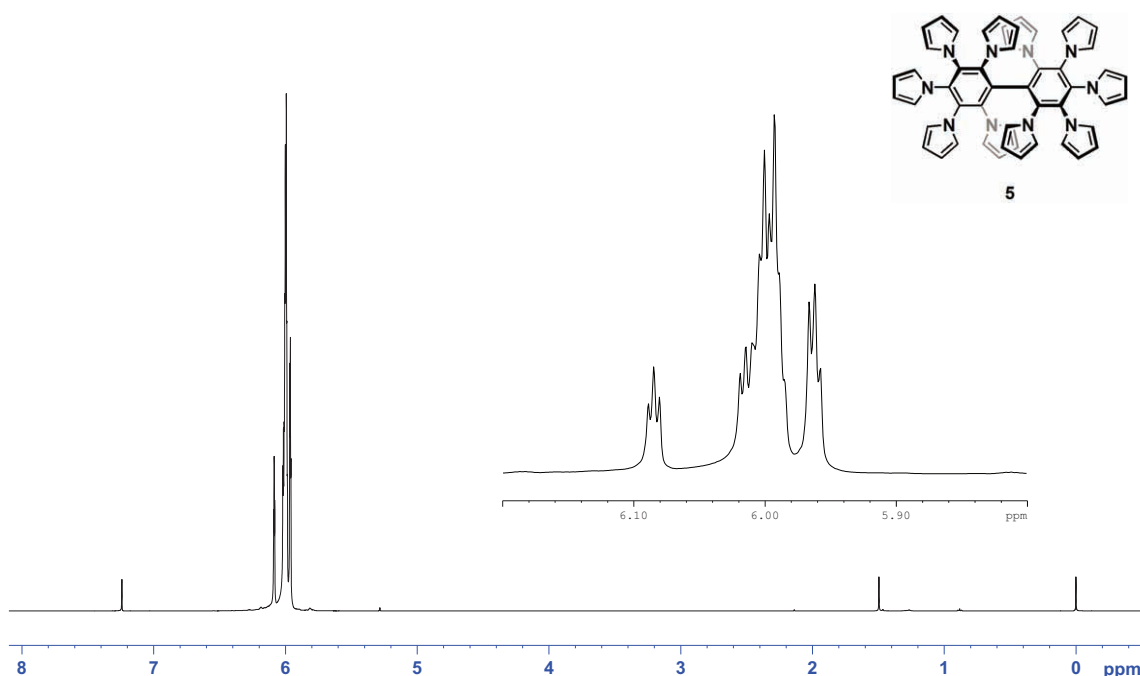
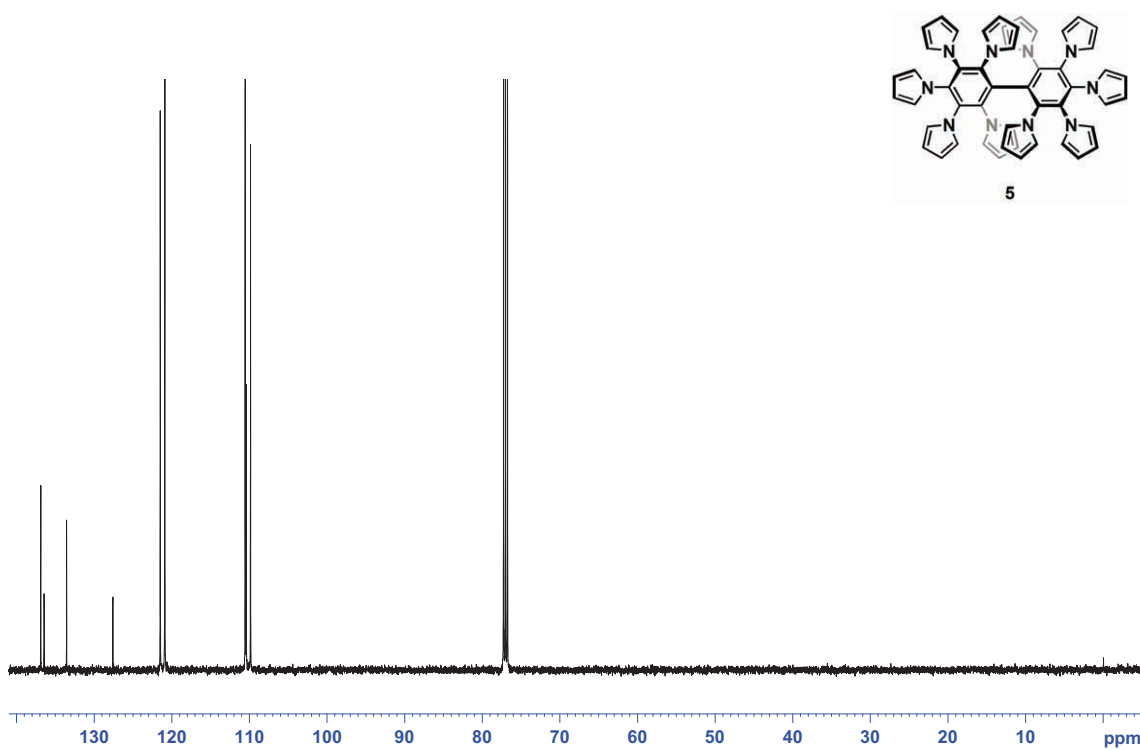
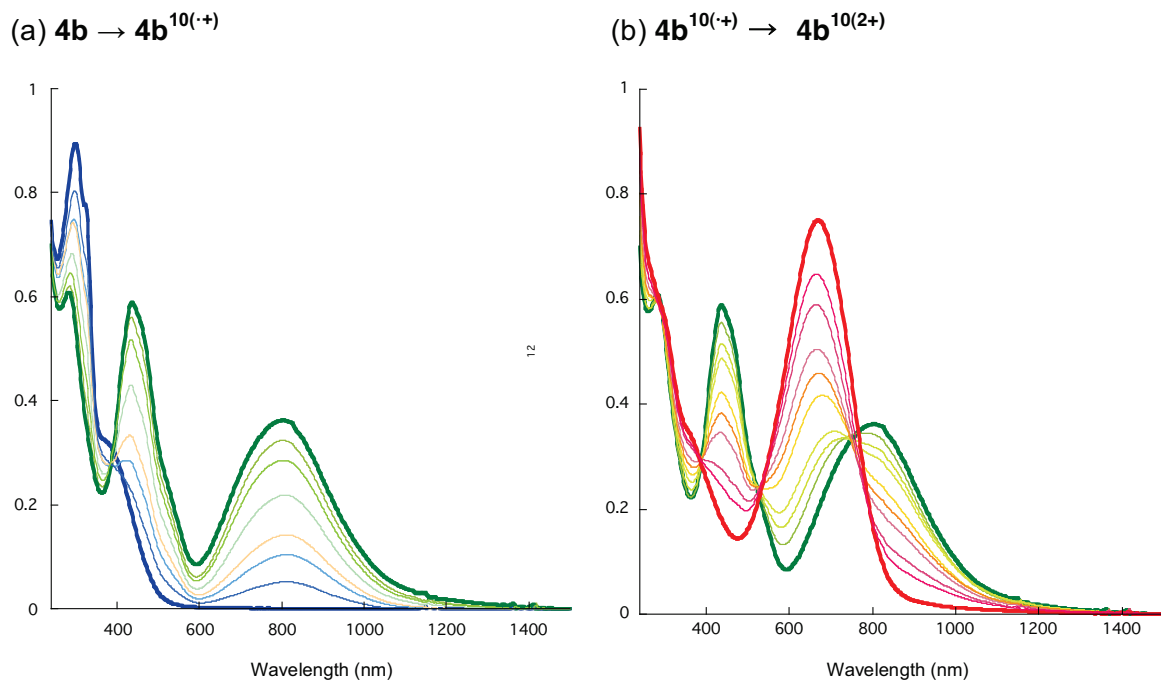


Figure S2-4. ^{13}C NMR of **5** (CDCl_3 , 125 MHz)



S3. Chemical oxidations of **4b**

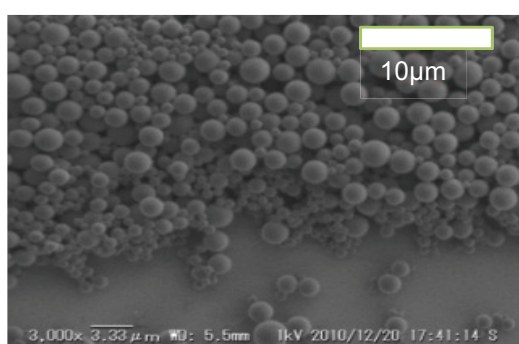
Figure S3-1. Absorption spectra of **4b** (0.02 mM) in the presence of various amount of oxidant, $\text{Fe}(\text{ClO}_4)_3 \bullet 6\text{H}_2\text{O}$ in a mixture of CH_2Cl_2 and CH_3CN (2:1, v/v) at room temperature.



S4. XRD patterns and SEM images of self-assembled **4b** and their conductivities

Figure S4-1. (a) SEM images and (b) XRD patterns of **4b-particle**. For SEM measurements, the samples were prepared by casting a suspension of nanostructures onto a cleaned Si wafer, followed by drying. The conductivities for these assembled structures were *measured by two-probe technique* using fine gold wires (10 μm diameter) attached to the pellets made of fibers, particles or films with carbon paste. Thickness of the pellets and spin coat films were estimated by AFM with tapping mode. The values are averages of two measurements by preparing different samples.

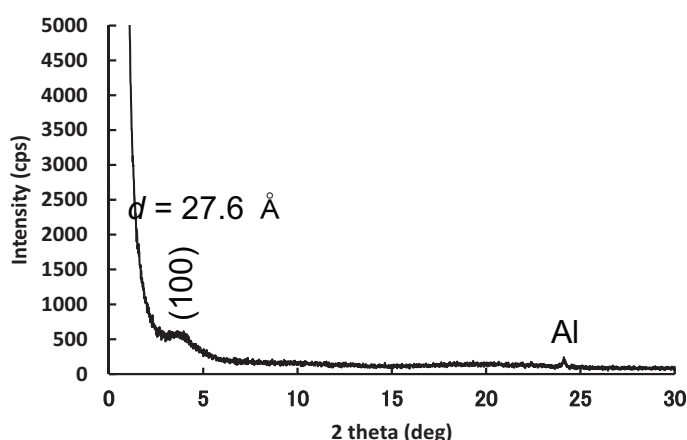
(a)



4b-particle: 5 mg/ml

(CH_2Cl_2 : hexane = 1:4, v/v)

(b)



$$\delta_{\text{rt}} = 7.8 \times 10^{-2} \text{ S/cm}$$

(after I_2 dope)

S5. Single crystal structure of 5

X-ray data were taken on a Bruker Smart APEX diffractometer equipped with a CCD area detector with graphite-monochromated MoKa. radiation ($\lambda = 0.71073 \text{ \AA}$). The structure was solved by direct methods (SHELXTL) and refined by the full-matrix least-squares method on F^2 (SHELXL-97). Non-hydrogen atoms were refined anisotropically, and hydrogen atoms were placed using AFIX instructions.

Figure S5-1. ORTEP drawings of 5.

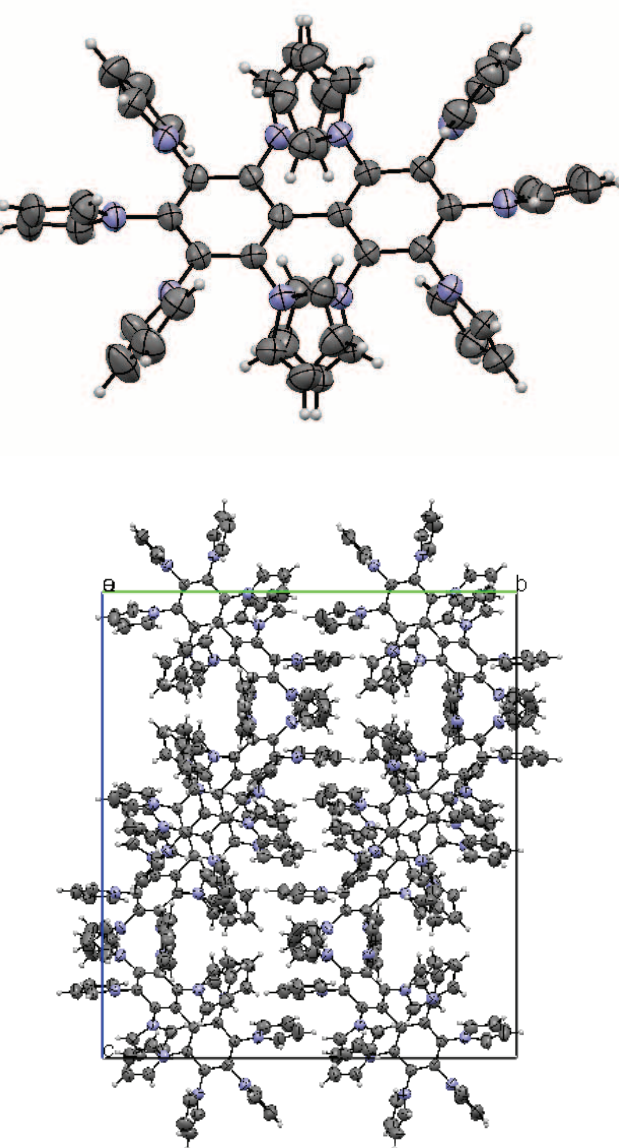


Table S5-1. Crystal data and structure refinement for **5**.

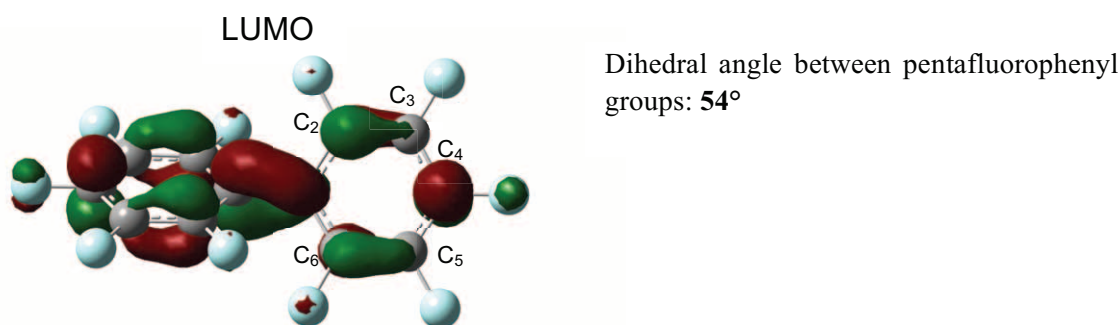
Identification code	5		
Empirical formula	C52 H40 N10		
Formula weight	804.94		
Temperature	293(2) K		
Wavelength	0.71073 Å		
Crystal system	orthorhombic		
Space group	Pbca		
Unit cell dimensions	$a = 14.853(3)$ Å	$\alpha = 90^\circ$.	
	$b = 22.747(3)$ Å	$\beta = 90^\circ$.	
	$c = 25.640(4)$ Å	$\gamma = 90^\circ$.	
Volume	8663(2) Å ³		
Z	8		
Density (calculated)	1.234 Mg/m ³		
Absorption coefficient	0.076 mm ⁻¹		
F(000)	3376		
Crystal size	0.40 x 0.20 x 0.30 mm ³		
Theta range for data collection	1.59 to 23.28°.		
Index ranges	-16≤h≤16, -25≤k≤22, -28≤l≤27		
Reflections collected	36688		
Independent reflections	6235 [R(int) = 0.0468]		
Completeness to theta = 23.28°	99.8 %		
Absorption correction	Empirical		
Refinement method	Full-matrix least-squares on F ²		
Data / restraints / parameters	6235 / 0 / 559		
Goodness-of-fit on F ²	1.035		
Final R indices [I>2sigma(I)]	R1 = 0.0431, wR2 = 0.1172		
R indices (all data)	R1 = 0.0686, wR2 = 0.1430		
Largest diff. peak and hole	0.151 and -0.214 e.Å ⁻³		

S6. DFT calculations of decafluorobiphenyl and **4a^[1]**

The optimizations were performed with D_2 symmetry for **4a** at the RB3LYP/6-31G (d) level of theory.

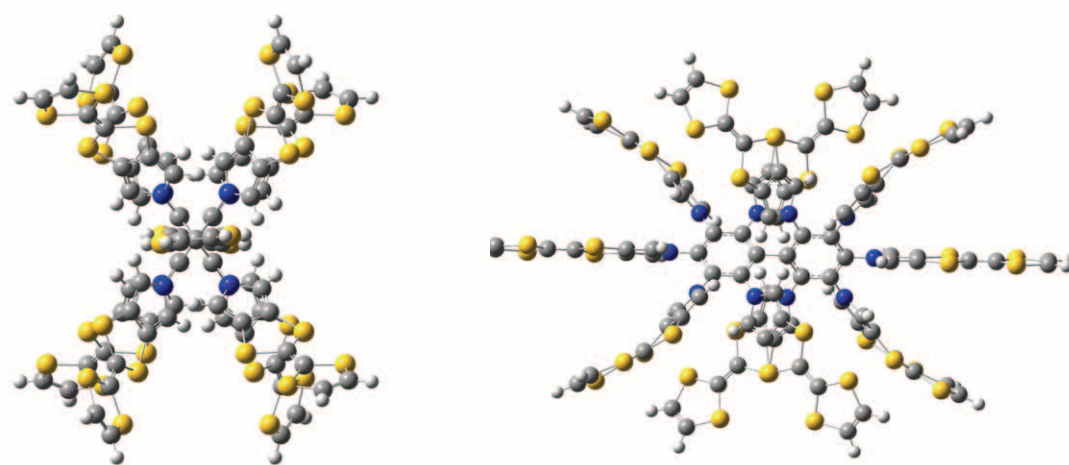
Figure S6-1. (a) LUMO of decafluorobiphenyl, and (b) optimized structure and (c) HOMO and LUMOs of **4a**.

(a) LUMO of decafluorobiphenyl



According to the LUMO of decafluorobiphenyl, the orbitals are preferentially located at the *ortho*- and *para*-positions (C_2 , C_2' , C_4 , and C_4'), indicating that the $S_{\text{N}}\text{Ar}$ reactions at these positions are favorable. However, once less hindered positions of the biphenyl moiety, *i.e.*, C_3 , C_3' , C_4 , C_4' , C_5 , and C_5' , are substituted, complete substitution at the *ortho*-positions, *i.e.*, C_2 , C_2' , C_6 , and C_6' , is hampered in the case with bulky substituent **6**, even at higher temperatures.

(b) Optimized structure of **4a**



Dihedral angle between the phenyl groups: **71°**

(c) Molecular orbitals of **4a**

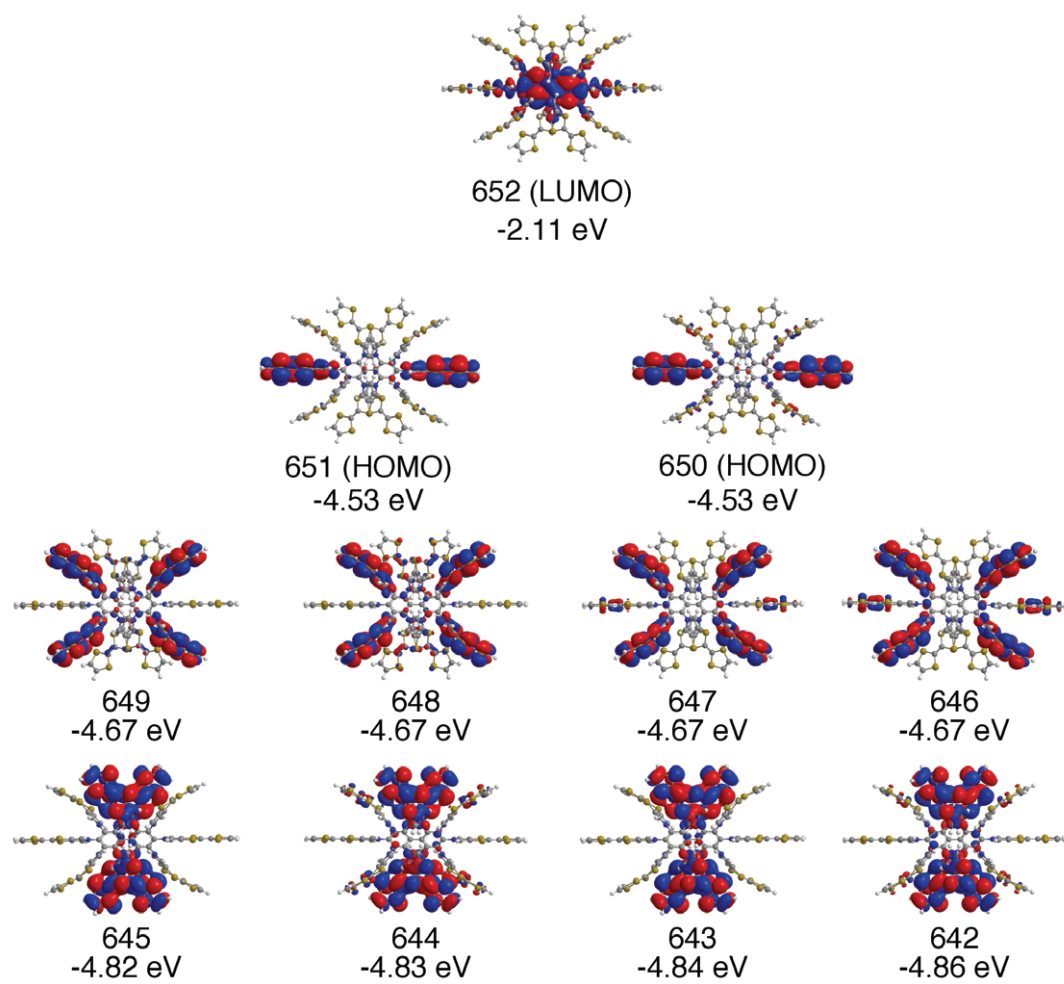


Table S8-1. Atomic coordination of **4a** (D_2 symmetry)

Center Number	Atomic Number	Coordinates (Angstroms)			63	16	3.198802	-8.047977	-2.308064
		X	Y	Z	64	16	4.716419	-6.031281	-3.909317
1	6	0.000000	0.000000	0.750307	65	7	-1.405379	2.023539	0.776464
2	6	-0.711951	0.990036	1.462852	66	6	-1.248528	3.383926	1.032351
3	6	-0.735648	0.974842	2.875487	67	6	-2.390561	1.855898	-0.201009
4	6	0.000000	0.000000	3.579419	68	6	-2.118789	4.061884	0.221062
5	6	0.735648	-0.974842	2.875487	69	1	-0.523328	3.734438	1.748412
6	6	0.711951	-0.990036	1.462852	70	6	-2.838852	3.101965	-0.551542
7	6	0.000000	0.000000	-0.750307	71	1	-2.672142	0.881833	-0.560967
8	6	-0.711951	-0.990036	-1.462852	72	16	-2.527910	5.757769	-0.032883
9	6	-0.735648	-0.974842	-2.875487	73	16	-4.060327	3.721791	-1.660142
10	6	0.000000	0.000000	-3.579419	74	6	-3.471388	5.411777	-1.517289
11	6	0.735648	0.974842	-2.875487	75	6	-3.751186	6.355101	-2.441672
12	6	0.711951	0.990036	-1.462852	76	16	-3.198802	8.047977	-2.308064
13	7	0.000000	0.000000	4.993587	77	16	-4.716419	6.031281	-3.909317
14	6	-1.132254	-0.116620	5.797075	78	7	-1.405379	-2.023539	-0.776464
15	6	1.132254	0.116620	5.797075	79	6	-2.390561	-1.855898	0.201009
16	6	-0.709424	-0.074009	7.100603	80	6	-1.248528	-3.383926	-1.032351
17	1	-2.117344	-0.189348	5.363811	81	6	-2.838852	-3.101965	0.551542
18	6	0.709424	0.074009	7.100603	82	1	-2.672142	-0.881833	0.560967
19	1	2.117344	0.189348	5.363811	83	6	-2.118789	-4.061884	-0.221062
20	16	-1.515265	-0.154121	8.660325	84	1	-0.523328	-3.734438	-1.748412
21	16	1.515265	0.154121	8.660325	85	16	-4.060327	-3.721791	1.660142
22	6	0.000000	0.000000	9.609790	86	16	-2.527910	-5.757769	0.032883
23	6	0.000000	0.000000	10.959239	87	6	-3.471388	-5.411777	1.517289
24	16	-1.490085	-0.158032	11.936945	88	6	-3.751186	-6.355101	2.441672
25	16	1.490085	0.158032	11.936945	89	16	-4.716419	-6.031281	3.909317
26	7	-1.480896	1.942837	3.589179	90	16	-3.198802	-8.047977	2.308064
27	6	-0.959351	2.839772	4.519266	91	7	-1.480896	-1.942837	-3.589179
28	6	-2.857057	2.132919	3.480626	92	6	-2.857057	-2.132919	-3.480626
29	6	-2.004756	3.593955	4.985394	93	6	-0.959351	-2.839772	-4.519266
30	1	0.089035	2.830833	4.773372	94	6	-3.195573	-3.149732	-4.334979
31	6	-3.195573	3.149732	4.334979	95	1	-3.448049	-1.545139	-2.795797
32	1	-3.448049	1.545139	2.795797	96	6	-2.004756	-3.593955	-4.985394
33	16	-2.163046	4.943186	6.106949	97	1	0.089035	-2.830833	-4.773372
34	16	-4.685550	4.004543	4.723751	98	16	-4.685550	-4.004543	-4.723751
35	6	-3.954683	4.867697	6.115152	99	16	-2.163046	-4.943186	-6.106949
36	6	-4.700099	5.454996	7.075027	100	6	-3.954683	-4.867697	-6.115152
37	16	-3.994850	6.354003	8.448513	101	6	-4.700099	-5.454996	-7.075027
38	16	-6.486660	5.420473	7.084857	102	16	-6.486660	-5.420473	-7.084857
39	7	1.480896	-1.942837	3.589179	103	16	-3.994850	-6.354003	-8.448513
40	6	0.959351	-2.839772	4.519266	104	7	1.405379	2.023539	-0.776464
41	6	2.857057	-2.132919	3.480626	105	6	2.390561	1.855898	0.201009
42	6	2.004756	-3.593955	4.985394	106	6	1.248528	3.383926	-1.032351
43	1	-0.089035	-2.830833	4.773372	107	6	2.838852	3.101965	0.551542
44	6	3.195573	-3.149732	4.334979	108	1	2.672142	0.881833	0.560967
45	1	3.448049	-1.545139	2.795797	109	6	2.118789	4.061884	-0.221062
46	16	2.163046	-4.943186	6.106949	110	1	0.523328	3.734438	-1.748412
47	16	4.685550	-4.004543	4.723751	111	16	4.060327	3.721791	1.660142
48	6	3.954683	-4.867697	6.115152	112	16	2.527910	5.757769	0.032883
49	6	4.700099	-5.454996	7.075027	113	6	3.471388	5.411777	1.517289
50	16	3.994850	-6.354003	8.448513	114	6	3.751186	6.355101	2.441672
51	16	6.486660	-5.420473	7.084857	115	16	4.716419	6.031281	3.909317
52	7	1.405379	-2.023539	0.776464	116	16	3.198802	8.047977	2.308064
53	6	1.248528	-3.383926	1.032351	117	7	1.480896	1.942837	-3.589179
54	6	2.390561	-1.855898	-0.201009	118	6	2.857057	2.132919	-3.480626
55	6	2.118789	-4.061884	0.221062	119	6	0.959351	2.839772	-4.519266
56	1	0.523328	-3.734438	1.748412	120	6	3.195573	3.149732	-4.334979
57	6	2.838852	-3.101965	-0.551542	121	1	3.448049	1.545139	-2.795797
58	1	2.672142	-0.881833	-0.560967	122	6	2.004756	3.593955	-4.985394
59	16	2.527910	-5.757769	-0.032883	123	1	-0.089035	2.830833	-4.773372
60	16	4.060327	-3.721791	-1.660142	124	16	4.685550	4.004543	-4.723751
61	6	3.471388	-5.411777	-1.517289	125	16	2.163046	4.943186	-6.106949
62	6	3.751186	-6.355101	-2.441672	126	6	3.954683	4.867697	-6.115152
					127	6	4.700099	5.454996	-7.075027
					128	16	6.486660	5.420473	-7.084857

129	16	3.994850	6.354003	-8.448513	157	6	-6.637357	6.108090	8.701781
130	7	0.000000	0.000000	-4.993587	158	1	-7.635702	6.178067	9.117603
131	6	1.132254	-0.116620	-5.797075	159	6	-4.369705	7.589841	-4.659296
132	6	-1.132254	0.116620	-5.797075	160	1	-4.744238	7.748762	-5.663711
133	6	0.709424	-0.074009	-7.100603	161	6	-3.691082	8.491290	-3.942346
134	1	2.117344	-0.189348	-5.363811	162	1	-3.434758	9.488127	-4.281596
135	6	-0.709424	0.074009	-7.100603	163	6	3.691082	8.491290	3.942346
136	1	-2.117344	0.189348	-5.363811	164	1	3.434758	9.488127	4.281596
137	16	1.515265	-0.154121	-8.660325	165	6	4.369705	7.589841	4.659296
138	16	-1.515265	0.154121	-8.660325	166	1	4.744238	7.748762	5.663711
139	6	0.000000	0.000000	-9.609790	167	6	5.523112	6.525692	-9.311337
140	6	0.000000	0.000000	-10.959239	168	1	5.487202	6.982929	-10.293237
141	16	1.490085	-0.158032	-11.936945	169	6	6.637357	6.108090	-8.701781
142	16	-1.490085	0.158032	-11.936945	170	1	7.635702	6.178067	-9.117603
143	6	6.637357	-6.108090	8.701781	171	6	-0.664730	0.070735	-13.490880
144	1	7.635702	-6.178067	9.117603	172	1	-1.280548	0.136144	-14.380265
145	6	5.523112	-6.525692	9.311337	173	6	0.664730	-0.070735	-13.490880
146	1	5.487202	-6.982929	10.293237	174	1	1.280548	-0.136144	-14.380265
147	6	-0.664730	-0.070735	13.490880	175	6	-5.523112	-6.525692	-9.311337
148	1	-1.280548	-0.136144	14.380265	176	1	-5.487202	-6.982929	-10.293237
149	6	0.664730	0.070735	13.490880	177	6	-6.637357	-6.108090	-8.701781
150	1	1.280548	0.136144	14.380265	178	1	-7.635702	-6.178067	-9.117603
151	6	-3.691082	-8.491290	3.942346	179	6	4.369705	-7.589841	-4.659296
152	1	-3.434758	-9.488127	4.281596	180	1	4.744238	-7.748762	-5.663711
153	6	-4.369705	-7.589841	4.659296	181	6	3.691082	-8.491290	-3.942346
154	1	-4.744238	-7.748762	5.663711	182	1	3.434758	-9.488127	-4.281596
155	6	-5.523112	6.525692	9.311337					
156	1	-5.487202	6.982929	10.293237					

S6. References

- [1] Gaussian 03, Revision E.01, Frisch, M. J.; Trucks, G. W.; Schlegel, H. B.; Scuseria, G. E.; Robb, M. A.; Cheeseman, J. R.; Montgomery, Jr., J. A.; Vreven, T.; Kudin, K. N.; Burant, J. C.; Millam, J. M.; Iyengar, S. S.; Tomasi, J.; Barone, V.; Mennucci, B.; Cossi, M.; Scalmani, G.; Rega, N.; Petersson, G. A.; Nakatsuji, H.; Hada, M.; Ehara, .; Toyota, K.; Fukuda, R.; Hasegawa, J.; Ishida, M.; Nakajima, T.; Honda, Y.; Kitao, O.; Nakai, H.; Klene, M.; Li, X.; Knox, J. E.; Hratchian, H. P.; Cross, J. B.; Bakken, V.; Adamo, C.; Jaramillo, J.; Gomperts, R.; Stratmann, R. E.; Yazyev, O.; Austin, A. J.; Cammi, R.; Pomelli, C.; Ochterski, J. W.; Ayala, P. Y.; Morokuma, K.; Voth, G. A.; Salvador, P.; Dannenberg, J. J.; Zakrzewski, V. G.; Dapprich, S.; Daniels, A. D.; Strain, M. C.; Farkas, O.; Malick, D. K.; Rabuck, A. D.; Raghavachari, K.; Foresman, J. B.; Ortiz, J. V.; Cui, Q.; Baboul, A. G.; Clifford, S.; Cioslowski, J.; Stefanov, B. B.; Liu, G.; Liashenko, A.; Piskorz, P.; Komaromi, I.; Martin, R. L.; Fox, D. J.; Keith, T.; Al-Laham, M. A.; Peng, C. Y.; Nanayakkara, A.; Challacombe, M.; Gill, P. M. W.; Johnson, B.; Chen, W.; Wong, M. W.; Gonzalez, C.; Pople, J. A. Gaussian, Inc., Wallingford CT, 2004.